

A combined proteomic and genetic analysis identifies a role for the lipid desaturase *Desat1* in starvation-induced autophagy in *Drosophila*

Katja Köhler,¹ Erich Brunner,² Xueli Guan,³ Karin Boucke,⁴ Urs F. Greber,⁴ Sonali Mohanty,² Julia M.I. Barth,¹ Markus R. Wenk³ and Ernst Hafen^{1,*}

¹ Institute of Molecular Systems Biology, Swiss Federal Institute of Technology Zürich, Zürich, Switzerland

² Center for Model Organism Proteomes, University of Zürich, Zürich, Switzerland

³ Department of Biochemistry and Department of Biological Sciences, Yong Loo Lin School of Medicine, National University of Singapore, Singapore

⁴ Institute of Zoology, University of Zürich, Zürich, Switzerland

key words: autophagy, *Drosophila*, proteome, lipids

Acknowledgments:

We thank Angela Baer and Anni Strässle for technical support, the members of the Hafen lab for helpful discussions and valuable suggestions, and the Bloomington stock center for fly stocks. This work was supported by grants from the Swiss National Science foundation.

Abbreviations: GFP, green fluorescent protein, FRT, flip recombinase target TEM, transmission electron microscopy, PBS, phosphate-buffered saline, PE, phosphatidylethanolamin, PC, phosphatidylcholine, PI, phosphatidylinositol, PL, phospholipids, RFP, red fluorescent protein, WT, wildtype.

Abstract:

Autophagy is a lysosomal-mediated degradation process that promotes cell survival during nutrient-limiting conditions. However, excessive autophagy results in cell death. In *Drosophila*, autophagy is regulated nutritionally, hormonally and developmentally in several tissues, including the fat body, a nutrient-storage organ. Here we use a proteomics approach to identify components of starvation-induced autophagic responses in the *Drosophila* fat body. Using clCAT() labeling and mass spectrometry, differences in protein expression levels of normal compared to starved fat bodies were determined. Candidates were analyzed genetically for their involvement in autophagy in fat bodies deficient for the respective genes. One of these genes, *Desat1*, encodes a lipid desaturase. *Desat1* mutant cells fail to induce autophagy upon starvation. The *desat1* protein localizes to autophagic structures after nutrient depletion and is required for fly development. Lipid analyses revealed that *Desat1* regulates the composition of lipids in *Drosophila*. We propose that *Desat1* exerts its role in autophagy by controlling lipid biosynthesis and/or signaling necessary for autophagic responses.

Running title: Proteomic analysis of starvation-induced autophagy

Introduction:

Autophagy has been described as a lysosomal degradation pathway for cytoplasmic material.¹ In response to starvation or other stresses, autophagy initiates with the formation of a flat membrane cisterna called the isolation membrane (IM) that engulfs cytosol and organelles. Sealing of the edges results in a double-membrane vesicle termed autophagosome that matures by fusing with lysosomes to form autolysosomes where degradation of the content occurs.² The recycling of amino acids and other nutrients from the digested material provides the cell with energy to survive starvation periods.

Autophagy is well conserved in all eukaryotic organisms, and functional homologues of most genes required for autophagy in yeast (Autophagy-related genes, Atg) have also been found in other species, such as *C. elegans*, *Drosophila* and mammals.¹ However, although the autophagic machinery is highly conserved, regulation of autophagy differs among and within various species. Autophagy plays a major role during development of multicellular organisms, in life-span extension and cell growth.³ It may also play a protective role against various human diseases, including cancer, neurodegenerative disorders, and microbial and viral infections.⁴ In addition to its role during cell survival, autophagy also promotes a type of cell death that is distinct from apoptosis, termed type II programmed cell death. Autophagic cell death first was observed in insects, but later was shown to be important during development of diverse organisms including humans. In *Drosophila*, autophagy has been described initially in salivary glands to be responsible for the programmed cell death of these organs during development.³ This death is triggered by the steroid hormone ecdysone and involves apoptotic as well as autophagic regulators.⁵⁻⁷ This has led to the hypothesis that autophagy and apoptosis can be interconnected, and sometimes even simultaneously regulated by the same trigger, resulting in different cellular outcomes. In other settings, autophagy may antagonize and protect cells from apoptotic death.

This brought up the idea of molecular switches between these two pathways. One such regulator is Beclin 1, an autophagic protein that binds the antiapoptotic molecule Bcl-2. The interaction with Bcl-2 was suggested to keep Beclin 1 function in check to prevent cells from excessive and thus lethal autophagy.⁸

Autophagy was also described in the fat body, an organ that, together with a specific set of cells called oenocytes,⁹ represents the liver analog of *Drosophila*.^{10,11} During larval development, the fat body undergoes massive growth driven by the nutrient-responsive Insulin/PI3K and target of rapamycin (TOR) signaling pathways. Inactivation of these pathways by removing dietary proteins inhibits growth, leading to a marked increase in autophagy in the larval fat body. PI3K and TOR signaling are able to suppress autophagic responses in the fat body, and autophagy is required to maintain cell size and survival when TOR is lacking.¹⁰

Autophagy-defective cells exhibit a growth advantage over wildtype cells under conditions that induce autophagy, suggesting that autophagy is a negative regulator of growth in TOR signaling.¹² Interestingly, the fat body is the predominant organ to exhibit starvation-dependent autophagy. Since this organ is believed to control development and growth by secreting growth factors and nutrients as a response to the nutritional status, the fat body could use autophagy to maintain adequate haemolymph nutrient levels to promote survival during periods of starvation.¹⁰ Despite this starvation-induced autophagy, the fat body also undergoes autophagy at the end of its larval life, a process that is developmentally regulated by ecdysone signaling to remove fat body cells during metamorphosis. Ecdysone-induced autophagy in the fat body can be blocked by constitutive expression of PI3K signaling components. Thus, PI3K and TOR signaling play a general role in controlling autophagy.¹¹

Although many signaling pathways impinging on autophagy and the core proteins of the autophagic machinery have been discovered, the identification of additional proteins will be necessary to answer some of the still unresolved questions in the field. For example, although it is well established that TOR is the central

regulator of autophagy, and that autophagy induction occurs via Atg1, the targets of both proteins are unknown. One of the major questions in the field concerns the process of autophagosome formation, since neither the mechanism of vesicle formation nor the membrane source is known. Further, to date, no information about the lipid composition of autophagosomal membranes has been gathered, and the role of lipids in autophagy remains unclear. Only recently, the first lipids involved in autophagic signaling have been identified.^{13,14} Finally, it is unclear which fusion components operate during autophagy, and how the autophagolysosomal vesicle is eventually broken down.

In this report, we perform a novel proteomics-based screen to search for candidates implicated in starvation-induced autophagy by comparing protein expression in fat bodies derived from starved and fed animals. Our data present the first quantitative proteomic analysis of starvation-induced autophagy in the *Drosophila* fat body. The subsequent genetic characterization of candidates in mutant and transgenic animals identified a desaturase (*Desat1*) to be important for autophagy. We show that *Desat1* has a crucial role in desaturation and biosynthesis of phospholipids. This data provides novel insights into the role of lipid biosynthesis and signaling necessary for autophagic processes.

Results:

Identification of proteins involved in starvation-induced autophagy.

In order to identify new components of starvation-induced autophagic responses, we performed a proteomic approach to compare protein levels in fat bodies from normal and starved larvae (Fig. 1A). Total protein was extracted from fat bodies isolated from larvae raised on normal food and from starved larvae. The two protein fractions were then differentially labeled with either light (normal) or heavy (starved) cLCATM reagent. After a proteolytic digest of the combined samples, the labeled peptides were isolated, analyzed by reverse-phase chromatography based tandem mass spectrometry (LC-MS/MS) and the resulting tandem-mass spectra searched against a standard *Drosophila* database as described in Brunner et al.¹⁵ Quantification of the cLCATM-derivatized peptides was achieved using the XPRESS software as described in Han et al.¹⁶ This led to the identification of a total of 214 proteins of which 41 were upregulated (ratio heavy/light >1.5) and 69 were downregulated (ratio heavy/light >0.8) in the starved sample. The complete list of proteins is freely available upon request to the authors. Upon the proteins upregulated under starvation, we identified CG5887, encoding Desat1, the fly homologue of the mammalian delta9 stearoyl-CoA desaturase (SCD). SCD catalyzes the desaturation of stearoyl- and palmitoyl-CoA to generate monounsaturated fatty acids (MUFA) that are incorporated into triglycerides, cholesteryl esters and membrane phospholipids.¹⁷ In *Drosophila*, Desat1 was shown to be implicated in sex pheromone production.¹⁸ However, a role of Desat1 under starvation conditions was not reported so far. To determine whether the identified proteins are involved in autophagy, larvae deficient for selected candidate genes were assayed for autophagic responses using lysotracker, a fluorescent dye staining autophagolysosomes. Only proteins of the upregulated

group were considered, and candidates were selected by their level of upregulation (>1.8) and the number of peptides identified (>2 independent identifications). While starvation induced strong lysotracker staining in the fat body of wild-type larvae, no lysotracker staining was observed in larvae homozygous mutant for the autophagy gene *Atg18* that served as a control in our assay (Fig. 1B). Of the candidates tested, only *Desat1* showed an effect on lysotracker staining. Since no flies mutant for *Desat1* were available, we used a *Desat1* RNAi line specifically activated in the fat body in combination with a heterozygous deficiency covering the *Desat1* gene. In fat bodies of these larvae, starvation led to a strong reduction in lysotracker staining, indicative of disturbed autophagy.

Generation and characterization of *Desat1* mutants.

The data so far suggested that *Desat1* is involved in starvation responses and autophagy. To further characterize *Desat1* function, we generated deletion mutants by imprecise excision of a P-element located 792 bp upstream of the ATG of the *Desat1* locus (P{EPgy2} *desat1*EY07679). The resulting alleles are shown in Figure 2A. The largest deletion 11A comprises the first three coding exons and part of the fourth coding exon, deletion 119A lacks the entire first coding exon, whereas deletion 28B lacks only the first 42 bp of coding exon 1. The coding region of *Desat1* contains two alternative ATGs downstream of the transcriptional start, which could be used to express a truncated protein in the deletions 119A and 28B. A precise excision of the P-element without disturbing the *Desat1* locus was also retrieved from the screen that served as a control for further experiments. Homozygosity for allele 11A or 119A and heteroallelic combination of the two deletions resulted in larval lethality with larvae dying during the second larval instar stage (L2), where they remained for up to 3 days without being able to moult into L3 (Fig. 2B). Very few (<5%) escapers were able to develop until larval stage 3, albeit

dramatically reduced in size, but no development beyond that stage could be observed. Further, the L2 larvae stop feeding and leave the yeast food source, a phenotype that was recently described in larvae where oenocytes, hepatocyte-like cells that regulate lipid metabolism and larval development were ablated. Interestingly, *Desat1* is expressed in oenocytes and was shown to physically interact with *Cyp4g1*, a gene important for lipid metabolism in oenocytes.⁹

In contrast, larvae homozygous for the deletion 28B developed normally, the resulting flies were fertile and did not show any obvious phenotype, indicating that *Desat1* function is not disturbed. To analyze protein expression in the mutants, we raised polyclonal antibodies against the C-terminus of *Desat1* and examined protein expression in larvae homozygous for the deletions by western blotting. As shown in Figure 2C, larvae homozygous for deletions 11A or 119A did not express any *Desat1* protein, whereas a protein of 44 kDa was expressed in control larvae. Larvae homozygous for allele 28B expressed a protein of around 30 kDa, corresponding to the expected size when the alternative ATG in exon 1 is used (Fig. 2C). Since flies homozygous for allele 28B were viable and fertile without any noticeable phenotype, we conclude that the N-terminus of *Desat1* is not important for its function.

In order to verify that the loss of *Desat1* function is responsible for the mutant phenotype, we carried out rescue experiments to restore viability of *Desat1* mutants by overexpressing the coding sequence (*cds*) of *Desat1* using UAS-driven transgenes in combination with various Gal4 drivers. Interestingly, overexpression of *Desat1* with the strong ubiquitous drivers actin-Gal4 or daughterless-Gal4 in a wild-type background led to lethality (data not shown). Using actin-Gal4, a few escapers (5% of the expected flies) hatched, albeit with a developmental delay of 3–4 days, leading to animals with reduced body size that died soon after hatching (data not shown). These data indicate that ubiquitous overexpression of *Desat1* is detrimental for some cells. However, when *Desat1* transgenes were overexpressed using the fat body specific driver *pumpless*-Gal4 (*ppl*-Gal4), flies developed normally

and hatched with the expected ratio (data not shown). Driving the expression of Desat1 using ppl-gal4 resulted in a partial rescue of the mutant lethality (22% of the expected flies hatching, data not shown). Using a genomic rescue construct containing 2.8 kb of the 5'UTR, the cds and 0.7 kb of the 3' UTR of the Desat1 locus led to 100% rescue of the lethality of Desat1 mutants, demonstrating that Desat1 function is indeed responsible for the observed phenotype (data not shown).

The loss of Desat1 function in flies leads to lethality, and ubiquitous overexpression of Desat1 interferes with fly development.

We thus wanted to determine whether Desat1 functions in cell death or cell survival using *Drosophila* cell culture. Indeed, downregulation of Desat1 by RNAi in S2 cells inhibited cellular growth

(Suppl. Fig. 1A and B). Flow cytometric analysis revealed that a significant fraction of the Desat1 knockdown cells lost the capacity to retain the dye DiOC6(3) and hence dissipated the mitochondrial transmembrane potential, a hallmark of apoptosis (Suppl.

Fig. 1C). A fraction of this cell population incorporated the vital dye propidium iodide and thus lost the plasma membrane barrier function, suggesting that Desat1 depletion sensitizes cells to death with apoptotic characteristics. On the other hand, overexpression of Desat1 in S2 cells also arrested cell growth (Suppl. Fig. 1D), however, no signs of cell death could be observed. Instead, proliferation was dramatically reduced in Desat1 overexpressing cells as monitored by BrDU incorporation assays (Suppl. Fig. 1E). Taken together, these results indicate that Desat1 function is necessary for cell survival and proliferation.

Desat1 is involved in autophagic processes. The lysotracker staining shown in Figure 1B suggested a role of Desat1 in autophagic responses in the fat body. In *Drosophila*, autophagy is regulated by various stresses, such as starvation or hypoxia, but is also under hormonal control by the steroid hormone ecdysone. Thus, the analysis and comparison of autophagy in tissues from different animals may be problematic and may not lead to conclusive results. In order to overcome confounding effects from those systemic influences, we analyzed the effect of Desat1 mutations on

autophagy in clones of cells by using surrounding wild-type cells as a control. Mutant clones for the alleles obtained in our screen (see Fig. 2A) were induced by FLP-FRT recombination and the resulting clones were recognized by the loss of a GFP transgene present on the homologous chromosome. Using this technique, we determined starvation-induced autophagy for the *Desat1* deletion alleles by lysotracker staining. In clones homozygous mutant for deletion 11A, no lysotracker staining was observed, while in the surrounding WT tissue, autophagy was induced upon 4 h sucrose starvation (Fig. 3A–A’). Similar results were obtained for clones of the deletion 119A (data not shown). Conversely, clones mutant for deletion 28B show normal lysotracker staining, confirming that this deletion does not affect *Desat1* function (data not shown). We also assessed autophagy by monitoring the intracellular localization of Atg8, a widely used marker for autophagosomes. Autophagy induction leads to an accumulation of Atg8-positive dots in the cytoplasm of fat body cells.¹⁰ Whereas in WT cells, the typical 2–5 μm sized Atg8-positive structures representing autolysosomes were observed (Fig. 3B’, arrows), the RFP-Atg8 signal was diffusely distributed in the cytoplasm and the nucleus in the adjacent *Desat1* mutant cells (Fig. 3B–B’). In some of those cells, we detected small-sized (<0.5 μm) RFP-Atg8 positive dots (Fig. 3B’, arrowheads) that did not overlap with lysotracker staining, suggesting that early autophagosomal structures were able to form, but did not develop into mature autophagosomes or autophagolysosomes (data not shown). We further confirmed the effect of *Desat1* mutations on autophagy by transmission electron microscopy (TEM) of fat bodies from WT versus *Desat1* mutant larvae. Starvation results in an increase in size and abundance of lysosomes that are filled with partially degraded material or intact organelles such as mitochondria, thereby identifying them as autolysosomes.¹⁰ Following 4 h of sucrose starvation, many autolysosomes were observed in control larval fat body cells (Fig. 3C, arrows and C’), whereas *Desat1* mutant fat body cells exhibited a strong reduction of these autophagic structures (Fig. 3D). In fact, starved *Desat1* mutant fat

body cells are rich in endoplasmatic reticulum and small lysosomes (Fig. 3D and D' arrowheads), features that have been described for nonstarved tissue.¹⁰ The Desat1 mutant cells were filled with small, electron-dense vesicles that were not present in WT cells. Most of these vesicles appeared to be ribosome-coated (see inset Fig. 3D'). These structures should not be considered autophagosomes, since autophagosomal membranes do not contain ribosomes.¹⁹ Instead, rough ER can form ring-shaped structures, suggesting that the disruption of the ER by mutations in Desat1 could result in these structures.

We further used the TEM data for quantification of the autophagic defect seen in Desat1 mutant cells.¹¹ Since typical autophagosomal structures were lacking, we quantified those cytoplasm-containing vesicles prominent in Desat1 mutant cells that were not ribosome-coated. Although the nature of these vesicles is unclear, they could represent aberrant autophagosomal structures resulting from the loss of Desat1 function, as suggested by the appearance of small Atg8-positive structures observed in Desat1 mutant cell clones (see Fig. 3B–B"). Taking into account all vesicles that possibly represent autophagosomal structures, this morphometric analysis revealed a strong reduction of the autophagic area in Desat1 mutant fat body cells compared to WT cells (Fig. 3E).

Taken together, these results indicate that cells lacking Desat1 function are severely impaired in their ability to induce autophagy under starvation.

Furthermore, we analyzed the intracellular localization of Desat1 in *Drosophila* S2 cells. Desat1 is expressed mainly in the ER under normal conditions; however, under starvation, we also observed Desat1 expression in intracellular vesicles and in close proximity to vacuolar structures. We thus tested whether Desat1 localizes to structures that are positive for Atg8 or Atg5 in starved S2 cells. Indeed, Desat1 expression was found on intracellular vesicles that were stained with GFP-Atg5 (Fig. 4A–A") and GFP-Atg8 (Fig. 4B–B"), suggesting that Desat1 partially localizes to autophagic structures under nutrient depletion.

Role of Desat1 in the biogenesis of membrane lipids. The Desat1 mammalian homologue SCD was shown to be a rate-limiting enzyme in lipogenesis. In mice, where several SCD isoforms exist, *Scd1*^{-/-} deficiency modulates the total levels and fatty acid composition of several phospholipid species.²⁰ The FA composition of phospholipids is tightly regulated and believed to influence membrane fluidity and the function of membrane proteins, thus regulating signal transduction.²¹ We therefore wondered whether Desat1 regulates lipid compositions in *Drosophila* and whether this regulation might be important for autophagy.

To determine the impact of Desat1 on lipid biosynthesis, we quantified the major fly phospholipids by mass spectrometry. Phosphatidylethanolamine (PE) was shown to be the major phospholipid in *Drosophila* tissues, followed by phosphatidylcholine (PC) and phosphatidylinositol (PI), whereas phosphatidylserine (PS) constitutes only a minor portion of total fly lipids.²² Thus, we focused on PE, PC and PI and analyzed lipid species containing Palmitic/Palmitoleic or stearic/oleic fatty acyl chains since palmitoyl-CoA and stearoyl-CoA are the preferred substrates of SCD.²³ Using multiple monitoring reaction based on headgroups and fatty acyl compositions of the lipid species, we detected a decrease in PC levels in Desat1 mutants and changes in the saturation profile of the major PC lipid species (Fig. 5A). PC species containing unsaturated fatty acyl chains were decreased in Desat1 mutants, whereas those comprised of saturated fatty acids were slightly increased, confirming the desaturase activity of Desat1. Detailed fatty acid analysis of PE lipids revealed that the species containing either 16:1 or 18:1 fatty acyl chains were decreased (Fig. 5B and B'), except 16:0/16:1 which showed no change and 18:0/18:1 which was increased in Desat1 mutants. Similarly, PI species containing one double bond at either position 16 or 18 were reduced in Desat1 mutants, except 16:0/16:1 and 16:1/18:0 and 18:0/18:1 which were increased (Fig. 5C and C'), possibly due to a highly specific substrate specificity of the desaturase. Nonetheless, for all phospholipids analyzed, species containing only saturated fatty acids were increased in Desat1 mutants. Taken together, these results

indicate that Desat1 affects the total levels and fatty acid composition of several phospholipid species in *Drosophila*.

SCD1 has also been shown to regulate ceramide levels, however, the nature of this regulation remains unclear as both a decrease or an increase in ceramide levels after SCD1 depletion were reported.^{20,24} The signaling pool of ceramides is produced either by de novo synthesis or by sphingomyelin hydrolysis. We thus analyzed ceramide and PE-ceramide (the fly analogue of sphingomyelin) levels in Desat1 mutant versus WT larvae. Both ceramides and PE-ceramides were elevated in Desat1 mutant larvae (Fig. 5D). Interestingly, ceramides can trigger both apoptosis and caspase-independent cell death, depending on the cellular context and stimuli.²⁵ It has been proposed that cells are sensitized to ceramide-induced death when autophagy is blocked.²⁶ Thus, if autophagy cannot proceed in cells lacking Desat1 function, elevated ceramide levels could be responsible for the cell death observed upon Desat1 depletion (see Suppl. Fig. 1).

Discussion

The cLCATM method reveals candidate proteins involved in autophagy. In this paper, we aimed to detect changes in protein expression during starvation-induced autophagy via a proteomics approach.

Gene expression

analyses in *Drosophila* using a variety of experimental conditions or developmental transitions in which autophagic responses are observed have been reported previously.^{5,6,27,28} In addition, a proteomic analysis has been carried out recently to identify proteins expressed during steroid-triggered autophagic cell death in salivary glands.⁷ However, a comparison of the results with our data is not entirely conclusive due to the variation

of the experimental setups, using different tissues, autophagic stimuli and developmental stages. Further, it seems impossible to separate autophagy from the numerous cellular processes other than autophagy, that allow cells to respond to changes in environmental or developmental conditions. Thus, we did not opt for a comparison of our screen with the ones published previously, and suggest the data to be considered as a list of candidate proteins putatively involved in starvation-induced autophagy in the fat body.

In our assay, we aimed to detect changes in protein expression after 4 h of autophagy induction, expecting to monitor early events of autophagic responses. In accordance with this, we identified many proteins regulating protein synthesis, e.g., translation initiation factors. Since starvation generally decreases protein synthesis, the translational regulators identified in our screen could represent promising candidates specifically implicated in the regulation of proteins necessary for autophagic processes. Interestingly, we found a variety of proteins to be upregulated that are implicated in lipid metabolism, including Desat1, which we further characterize in this paper. One might speculate that these enzymes may be involved in the generation of lipids necessary for autophagosome formation, or implicated in lipid signaling to trigger autophagy.

Desat1 was not found to be transcriptionally regulated during autophagy.^{5,6,27,28} The fact that we detected an upregulation of Desat1 protein upon starvation suggests that Desat1 is likely to be regulated translationally under these conditions. In line with this, we observed that knocking down Desat1 by RNAi does not decrease Desat1 mRNAs, whereas Desat1 protein expression is completely abolished (data not shown). This suggests that

controlling protein expression rather than transcription could regulate Desat1 function. Thus, our proteomic approach potentially revealed new players of autophagic responses that could not be identified in the previous screens where mainly transcription profiles were determined.

Desat1 plays a role in autophagic processes. The upregulation of Desat1 protein under starvation in our proteomic approach suggested a role for this protein in autophagy. Indeed, Desat1 mutant cells fail to induce autophagy and lack typical autophagic structures, indicating that Desat1 is necessary for autophagic responses. Based on its enzymatic function, the observed changes in the lipid profiles of Desat1 mutants and the association of Desat1 with ER and autophagosomes, we favor the hypothesis that Desat1 acts on autophagic processes by regulating lipid biosynthesis. One possibility is that Desat1 is implicated in the production of lipid species that are necessary either for the induction of autophagy or for the generation of autophagic membranes. Unfortunately, the lipid composition of autophagosomes remains still unknown; thus, no conclusion about the involvement of Desat1 in the synthesis of autophagosome-specific lipids can be drawn.

A still unsolved issue in autophagic processes concerns the origin of the autophagic membranes and the mechanism of autophagosome formation.³⁰ Upon autophagy induction, the isolation membrane (IM) engulfs parts of the cytoplasm to form the autophagosome.² Two general models of IM expansion are currently considered. According to the maturation model, preexisting organelle membranes are delivered to the IM, whereas in the assembly model, autophagosomal membranes would assemble de novo from localized lipid synthesis or transport. Although multiple organelles may be involved in supplying membranes for autophagosome formation, a likely main source is the ER. This is supported by a similar membrane thickness of autophagosomes and ER membranes and the identification of ER proteins in IMs and autophagosomes.³¹ Further, it was shown in yeast that genes involved in ER trafficking are required for autophagy.³² If the maturation model is correct, a part of the ER may fold

itself to form the IM, or vesicle may bud off from the ER and fuse to generate the IM. There may exist uniquely differentiated regions at the ER from which the IM generate, e.g., by coating the membranes with the Atg proteins necessary for autophagosome formation and expansion.³³ Interestingly, it was shown recently in an elegant study that autophagosome formation takes place at membrane compartments enriched in PI3P that are dynamically connected to the ER (called omegasomes),³⁴ further supporting the idea that the ER provides the membranes needed for autophagosome biogenesis.

Our data provide additional evidence that the ER plays an important role in generating membrane material during autophagy. We show that Desat1, an integral ER membrane protein, localizes to autophagic structures upon starvation. This translocation from the ER to a punctate compartment which partially colocalized with autophagosomal markers has also been observed for DFCP1, a protein that localizes to the PI3P-enriched omegasomes involved in autophagosome biogenesis mentioned above.³⁴ Since DFCP1 colocalizes with Atg5 and Atg8, components of the two conjugation systems required for autophagosome formation, it was suggested that omegasomes could represent platforms for the nucleation of IM with the ER providing the lipids needed for the conjugation step. A similar scenario could be envisaged for Desat1. Desat1 may establish microdomains on the ER from which autophagy can proceed, e.g., by generating special lipid species to locally modulate membrane characteristics, such as curvature or fluidity, to facilitate autophagy induction. The membrane curvature necessary for autophagosome formation was suggested to be controlled by the Atg5-Atg12/Atg16 complex to favor the ordered assembly of Atg8-PE.³³ Alternatively, the membrane curvature could also be generated by the controlled insertion of lipid species into IMs. In this respect, it was shown that changing acyl chain compositions, such as elongation and desaturation, serve to adjust membrane curvature.³⁵ Lipid species generated by Desat1 could be inserted into lipid bilayers to influence the curvature of membranes implicated in the formation of autophagosomes.

Additionally, Desat1 could control membrane fluidity at the sites of autophagosome formation. Membrane fluidity is determined by the quantity and distribution of saturated and unsaturated fatty acids and influences the function of transporters and receptors to control signal transduction. The mammalian Desat1 homologue SCD was shown to regulate the biophysical properties of membranes by altering phospholipid fatty acid composition.³⁶ Since our lipid analysis has shown that Desat1 is a major regulator of desaturation in *Drosophila*, the fluidity of membranes and thus signaling during autophagic processes could be controlled by the regulated expression of Desat1.

In addition to the profound alterations in fatty acid distribution in the main phospholipid fractions promoted by Desat1 depletion, the synthesis of various PC, PI and PE species was significantly reduced in Desat1 deficient larvae. This provides evidence that Desat1 may play a role not only in the regulation of fatty acid remodeling of preexisting membrane lipids, but also in the de novo synthesis of phospholipids. The induction of Desat1 expression under starvation may boost the synthesis of lipid species needed for autophagosome formation for example, PE used to covalently link ATG8 to pre-autophagosomal structures.³⁷ Further, PC is the primary phospholipid of eukaryotic cellular membranes and has a crucial role in structural maintenance of the lipid bilayer. PC is also the major component of intracellular transport vesicles, and PC participates in the regulation of vesicle trafficking to the yeast vacuole.³⁸ Thus, the generation of PC by Desat1 could be important to ensure the integrity of autophagic vesicles and/or their intracellular trafficking.

Alternatively, Desat1 could influence autophagy by controlling the production of lipid species that are implicated in autophagic signaling. For example, ceramide was shown to be a key regulator of apoptosis.³⁹ However, it was shown recently that ceramide is also able to induce autophagic cell death in nutrient-rich conditions.^{13,40} The mechanism by which ceramide regulates both apoptosis and autophagy is unclear, however, a recent study proposes that autophagy is a protective response to increasing ceramide

levels,²⁶ as blocking autophagy sensitizes cells to ceramide-induced death. Ceramide affects autophagy by activating the pro-apoptotic molecule Bnip3, and was also shown to induce *beclin 1* expression.^{13,40} The interaction of Beclin 1 with Bcl2 is believed to be required for maintaining autophagy in a physiological range to protect from autophagic cell death. However, disturbing the Beclin 1/Bcl2 complex may lead to excessive autophagy that promotes cell death.⁸ The ceramide-induced increase in Beclin 1 could change the ratio of Beclin 1/Bcl2 in a range incompatible with survival. Interestingly, the amounts of ceramide remain unchanged under starvation, suggesting that ceramide is mainly implicated in the regulation of autophagic death, and ceramide levels must be kept in check during starvation-induced autophagy.

The increase in ceramide and PE-ceramide levels in *Desat1* mutant larvae points to a negative regulatory role of *Desat1* in ceramide synthesis, most likely by controlling the substrate provision for the production of ceramides from sphingomyelin (PE-ceramide) hydrolysis. This would be compatible with a role for *Desat1* for survival by controlling ceramide levels involved in balancing autophagic responses.

On the other hand, ceramide and other lipids could play a structural role in autophagosome biogenesis. It is now established that ceramide is responsible for a negative curvature of the membrane.²⁵ The production of this lipid could be used to promote membrane curvature by trapping of ceramide on one leaflet of the membrane by phosphorylation, which is how ceramide participates for instance in phagocytosis.⁴¹

In conclusion, we have used a novel proteomics-based approach to reveal changes in protein expression during starvation-induced autophagy in *Drosophila*. We demonstrate that one of the identified proteins, *Desat1*, is required for autophagy. *Desat1* mutant larvae show dramatic changes in lipid compositions. Given the role of *Desat1* in regulating lipid biosynthesis, our data provides prospective hints on which lipid species may be implicated in autophagy, either during the formation of autophagosomes or as second messengers important for autophagic signaling.

Materials and Methods

Drosophila stocks and culture. The following fly stocks were obtained from the Bloomington stock center: *y w*; *act5C-Gal4*, *y w*; *ppl-Gal4*, *y w hsf1p*; *FRT82UbiGFP*, *Df(3R)Exel7316*, *y w*; *Atg18KG03090*, *y w*; *P{EPgy2}desat1EY07679*. The RNAi line *y w*; *P{GD2950}v33338* was obtained from the Vienna *Drosophila* RNAi center. The UAS-RFP-*Atg8* construct was generated in our laboratory. All crosses were performed at 25°C.

For the autophagy assays, flies were allowed to lay eggs for 2 h on standard cornmeal/molasses/agar fly food supplemented with fresh yeast paste. 72 h after egg laying, larvae were collected and put either in vials with standard food (normal) or in vials containing 20% sucrose in PBS (starved) for 4 h before dissection. Fat body clones were induced by heat shock 8 h after egg laying at 37°C for 1 h, and fat bodies were analyzed 72 h after egg laying as indicated above. Generation of RFP-*Atg8*. *Drosophila Atg8a* was PCR-amplified

from cDNA of *y w* flies. The PCR product was cloned using the Gateway system (Invitrogen) and transferred into the pTRW destination vector (The *Drosophila* Gateway Vector Collection, Carnegie Institution). The resulting UAS-RFP-*Atg8* construct was injected into *y w* embryos for transformation, and 3 transgenic lines on two different chromosomes were established and tested.

Generation of *Desat1* mutants. In order to generate *Desat1* mutants, the P-element *P{EPgy2}desat1EY07679* (marked with *w+*) inserted 792 bp upstream of the start codon of *Desat1* was mobilized by supplying D2-3 transposase. Jump starter males were mated with balancer females and single F1 *w-* males were recrossed to balancer virgins. Stocks were established and molecularly tested for deletions by single-fly PCR leading to the identification of the alleles *Desat11A*, *Desat119A* and *Desat28B*. A precise excision of the P-element without disturbing the *Desat1* locus was kept as a control for further experiments (*Desat10*).

Lysotracker assay. Fat body from fed or starved larvae was dissected in PBS and incubated for 1 min in 100 mM Lysotracker

red DND-99 (Molecular Probes #L7528) and 1 mM DAPI (Sigma #32670) in PBS. Fat bodies were then transferred on glass slides, covered and immediately photographed live on a Zeiss Axiophot fluorescent microscope.

Electron microscopy and quantification. Fat bodies were fixed for 1 h at 4°C with 2% glutaraldehyde and 1% OsO₄ in 100 mM cacodylate buffer, and postfixed in 2% OsO₄ in 100 mM cacodylate buffer for 2 h at 4°C. Samples were dehydrated in acetone and embedded in Spurr. 90 nm sections were cut and collected on Parlodion covered copper grids (SYNAPTEK, Electron Microscopy Sciences, #S2010-Not). Sections were stained in 4% aqueous uranyl acetate for 40 min, rinsed and stained with Sato triple lead stain for 20 min. Sections were viewed on a ZEISS EM10 transmission electron microscopy, photographed with a Erlangshen ES 500W camera and processed using the DigitalMicrograph software package from GATAN. Quantification of the autophagic area in the fat body cytosol was performed on fat bodies from two different animals for each experimental condition. 15–20 randomly chosen fields were photographed at 3125x magnification and the area occupied by autophagic structures was determined by pixel counting. Autophagic structures were scored according to their morphology, comprising all structures that contained recognizable cytosolic material. The amount of autophagic vesicles was calculated per 100 mm² cytosol and the data presented as mean values +/- SDE.

Western blotting. Five 2nd instar larvae of the respective genotypes were frozen in liquid nitrogen and lysed in lysis buffer (120 mM NaCl, 50 mM Tris-HCl, 1 mM EDTA, 6 mM EGTA, 1% Nonidet P-40) containing protease inhibitors (20 mM NaF, 1 mM Benzamidine, 15 mM NA4P2O₇ and Mini Protease Inhibitor Cocktail Tablets, Roche #11873580001). Proteins were separated on a 10% SDS PAGE gel and blotted onto a Nitrocellulose (Amersham #RPN303D) membrane. The membrane was incubated with rabbit anti-Desat1 (our lab, see below) and mouse anti-tubulin (Sigma #T9026) antibodies. After incubation with

anti-mouse or anti-rabbit HRP secondary antibodies (Jackson ImmunoResearch, #115-065-003, #111-035-003), blots were developed using the ECL Western Chemiluminescence Kit (Amersham #RPN2125).

The anti-Desat1 antibody was generated in rabbits against the last 15 c-terminal amino acids (QPKEEIEDAVITHKK) and affinity purified by Eurogentec (Brussels, Belgium).

clCATTM experiment. Larval fat bodies were obtained as for the autophagy assay. Fat bodies were isolated and protein extraction, clCATTM labeling and mass spectrometric analyses were performed as described in Brunner et al.¹⁵ Quantification was performed using the XPRESS software¹⁶ and each elution profile was manually curated.

Lipid analysis. 5 mg dry weight of larvae were extracted as described by modified Bligh-Dyer method,⁴⁵ and dilignoceroyl GPCho (Avanti Polar Lipids, #850573), dimyristoyl GPEtn (Avanti Polar Lipids, #850745), dioctyl GPIs (Echelon Biosciences, #P-0008), didocosahexaenoyl GPSer (Avanti Polar Lipids, #840067) and N-nonadecanoyl Ceramide (Matreya, #2039) were added as internal lipid standards. Quantification of individual molecular species was carried out using multiple reaction monitoring (MRM) with an Applied Biosystems 4000 Q-Trap mass spectrometer (Applied Biosystems) and amount of lipids is obtained by normalizing to relevant standards, with the following exception—to monitor the fatty acyl compositions of these lipids (parent→fatty acyl fragment transitions)—the signal intensity of each MRM value was normalized using the following equation:
Normalized intensity of lipid 1 = $\frac{\text{Signal intensity of lipid 1}}{\sum [\text{Signal intensity of all MRM transitions measured}]}$
Comparison of the means of wild type and mutants from three independent experiments was performed.⁴⁵

Acknowledgements

We thank Angela Baer and Anni Strässle for technical support, Ermir Qeli from the Center for Model Organism Proteomes for statistical analysis and the members of the Hafen lab for helpful

discussions and valuable suggestions. This work was supported by grants from the Swiss National Science foundation and by grants from the Singapore National Research Foundation under CRP Award No. 2007-04, the Biomedical Research Council of Singapore (R-183-000-211-305), the National Medical Research Council (R-183-000-224-213) and the SystemsX.ch RTD project LipidX.

References

1. Levine B, Klionsky DJ. Development by self-digestion: molecular mechanisms and biological functions of autophagy. *Dev Cell* 2004; 6:463-77.
2. Mizushima N, Yamamoto A, Hatano M, Kobayashi Y, Kabeya Y, Suzuki K, et al. Dissection of autophagosome formation using Apg5-deficient mouse embryonic stem cells. *J Cell Biol* 2001; 152:657-68.
3. Baehrecke EH. Autophagic programmed cell death in *Drosophila*. *Cell Death Differ* 2003; 10:940-5.
4. Orvedahl A, Levine B. Eating the enemy within: autophagy in infectious diseases. *Cell Death Differ* 2009; 16:57-69.
5. Gorski SM, Chittaranjan S, Pleasance ED, Freeman JD, Anderson CL, Varhol RJ, et al. A SAGE approach to discovery of genes involved in autophagic cell death. *Curr Biol* 2003; 13:358-63.
6. Lee CY, Clough EA, Yellon P, Teslovich TM, Stephan DA, Baehrecke EH. Genome-wide analyses of steroid- and radiation-triggered programmed cell death in *Drosophila*. *Curr Biol* 2003; 13:350-7.
7. Martin DN, Balgley B, Dutta S, Chen J, Rudnick P, Cranford J, et al. Proteomic analysis of steroid-triggered autophagic programmed cell death during *Drosophila* development. *Cell Death Differ* 2007; 14:916-23.
8. Pattingre S, Tassa A, Qu X, Garuti R, Liang XH, Mizushima N, et al. Bcl-2 antiapoptotic proteins inhibit Beclin 1-dependent autophagy. *Cell* 2005; 122:927-39.
9. Gutierrez E, Wiggins D, Fielding B, Gould AP. Specialized hepatocyte-like cells regulate *Drosophila* lipid metabolism. *Nature* 2007; 445:275-80.

10. Scott RC, Schuldiner O, Neufeld TP. Role and regulation of starvation-induced autophagy in the *Drosophila* fat body. *Dev Cell* 2004; 7:167-78.
11. Rusten TE, Lindmo K, Juhasz G, Sass M, Seglen PO, Brech A, et al. Programmed autophagy in the *Drosophila* fat body is induced by ecdysone through regulation of the PI3K pathway. *Dev Cell* 2004; 7:179-92.
12. Scott RC, Juhasz G, Neufeld TP. Direct induction of autophagy by Atg1 inhibits cell growth and induces apoptotic cell death. *Curr Biol* 2007; 17:1-11.
13. Scarlatti F, Bauvy C, Ventruti A, Sala G, Cluzeaud F, Vandewalle A, et al. Ceramidemediated macroautophagy involves inhibition of protein kinase B and upregulation of beclin 1. *J Biol Chem* 2004; 279:18384-91.
14. Lavieu G, Scarlatti F, Sala G, Carpentier S, Levade T, Ghidoni R, et al. Regulation of autophagy by sphingosine kinase 1 and its role in cell survival during nutrient starvation. *J Biol Chem* 2006; 281:8518-27.
15. Brunner E, Ahrens CH, Mohanty S, Baetschmann H, Loevenich S, Potthast F, et al. A high-quality catalog of the *Drosophila melanogaster* proteome. *Nat Biotechnol* 2007; 25:576-83.
16. Han DK, Eng J, Zhou H, Aebersold R. Quantitative profiling of differentiation-induced microsomal proteins using isotope-coded affinity tags and mass spectrometry. *Nat Biotechnol* 2001; 19:946-51.
17. Ntambi JM, Miyazaki M. Recent insights into stearoyl-CoA desaturase-1. *Curr Opin Lipidol* 2003; 14:255-61.
18. Marcillac F, Bousquet F, Alabouvette J, Savarit F, Ferveur JF. A mutation with major effects on *Drosophila melanogaster* sex pheromones. *Genetics* 2005; 171:1617-28.
19. Eskelinen EL. To be or not to be? Examples of incorrect identification of autophagic compartments in conventional transmission electron microscopy of mammalian cells. *Autophagy* 2008; 4:257-60.
20. Dobrzyn A, Dobrzyn P, Miyazaki M, Sampath H, Chu K, Ntambi JM. Stearoyl-CoA desaturase 1 deficiency increases CTP:choline cytidyltransferase translocation into the membrane and enhances phosphatidylcholine synthesis in liver. *J Biol Chem* 2005; 280:23356-62.
21. Ntambi JM. Regulation of stearoyl-CoA desaturase by polyunsaturated fatty acids and cholesterol. *J Lipid Res* 1999; 40:1549-58.
22. Stark WS, Lin TN, Brackhahn D, Christianson JS, Sun GY. Phospholipids in *Drosophila* heads: effects of visual mutants and phototransduction manipulations. *Lipids* 1993; 28:23-8.

23. Enoch HG, Strittmatter P. Role of tyrosyl and arginyl residues in rat liver microsomal stearylcoenzyme A desaturase. *Biochemistry* 1978; 17:4927-32.
24. Pinnamaneni SK, Southgate RJ, Febbraio MA, Watt MJ. Stearoyl CoA desaturase 1 is elevated in obesity but protects against fatty acid-induced skeletal muscle insulin resistance in vitro. *Diabetologia* 2006; 49:3027-37.
25. Zheng W, Kollmeyer J, Symolon H, Momin A, Munter E, Wang E, et al. Ceramides and other bioactive sphingolipid backbones in health and disease: lipidomic analysis, metabolism and roles in membrane structure, dynamics, signaling and autophagy. *Biochim Biophys Acta* 2006; 1758:1864-84.
26. Guenther GG, Peralta ER, Rosales KR, Wong SY, Siskind LJ, Edinger AL. Ceramide starves cells to death by downregulating nutrient transporter proteins. *Proc Natl Acad Sci USA* 2008; 105:17402-7.
27. Juhasz G, Puskas LG, Komonyi O, Erdi B, Maroy P, Neufeld TP, et al. Gene expression profiling identifies FKBP39 as an inhibitor of autophagy in larval *Drosophila* fat body. *Cell Death Differ* 2007; 14:1181-90.
28. Zinke I, Schutz CS, Katzenberger JD, Bauer M, Pankratz MJ. Nutrient control of gene expression in *Drosophila*: microarray analysis of starvation and sugar-dependent response. *EMBO J* 2002; 21:6162-73.
29. Juhasz G, Neufeld TP. Autophagy: a forty-year search for a missing membrane source. *PLoS Biol* 2006; 4:36.
30. Dunn WA Jr. Autophagy and related mechanisms of lysosome-mediated protein degradation. *Trends Cell Biol* 1994; 4:139-43.
31. Ishihara N, Hamasaki M, Yokota S, Suzuki K, Kamada Y, Kihara A, et al. Autophagosome requires specific early Sec proteins for its formation and NSF/SNARE for vacuolar fusion. *Mol Biol Cell* 2001; 12:3690-702.
32. Reggiori F, Klionsky DJ. Autophagosomes: biogenesis from scratch? *Curr Opin Cell Biol* 2005; 17:415-22.
33. Axe EL, Walker SA, Manifava M, Chandra P, Roderick HL, Habermann A, et al. Autophagosome formation from membrane compartments enriched in phosphatidylinositol 3-phosphate and dynamically connected to the endoplasmic reticulum. *J Cell Biol* 2008; 182:685-701.
34. Boumann HA, Gubbens J, Koorengel MC, Oh CS, Martin CE, Heck AJ, et al. Depletion of phosphatidylcholine in yeast induces shortening and increased saturation of the lipid acyl chains: evidence for regulation of intrinsic membrane curvature in a eukaryote. *Mol Biol Cell* 2006; 17:1006-17.

35. Sun Y, Hao M, Luo Y, Liang CP, Silver DL, Cheng C, et al. Stearoyl-CoA desaturase inhibits ATP-binding cassette transporter A1-mediated cholesterol efflux and modulates membrane domain structure. *J Biol Chem* 2003; 278:5813-20.
36. Sou YS, Tanida I, Komatsu M, Ueno T, Kominami E. Phosphatidylserine in addition to phosphatidylethanolamine is an in vitro target of the mammalian Atg8 modifiers, LC3, GABARAP and GATE-16. *J Biol Chem* 2006; 281:3017-24.
37. Howe AG, McMaster CR. Regulation of vesicle trafficking, transcription and meiosis: lessons learned from yeast regarding the disparate biologies of phosphatidylcholine. *Biochim Biophys Acta* 2001; 1534:65-77.
38. Pettus BJ, Chalfant CE, Hannun YA. Ceramide in apoptosis: an overview and current perspectives. *Biochim Biophys Acta* 2002; 1585:114-25.
39. Daido S, Kanzawa T, Yamamoto A, Takeuchi H, Kondo Y, Kondo S. Pivotal role of the cell death factor BNIP3 in ceramide-induced autophagic cell death in malignant glioma cells. *Cancer Res* 2004; 64:4286-93.
40. Hinkovska-Galcheva VT, Boxer LA, Mansfield PJ, Harsh D, Blackwood A, Shayman JA. The formation of ceramide-1-phosphate during neutrophil phagocytosis and its role in liposome fusion. *J Biol Chem* 1998; 273:33203-9.
41. Guan XL, Wenk MR. Mass spectrometry-based profiling of phospholipids and sphingolipids in extracts from *Saccharomyces cerevisiae*. *Yeast* 2006; 23:465-77.

Figures and figure legends:

Figure 1. Identification of proteins involved in starvation-induced autophagy using a proteomics approach. (A) Overview of the cLCATM experiment on larval fat bodies. (B) Verification of the candidates using the autophagic marker lysotracker. Starvation induces lysotracker staining in WT, but not in *Atg18^{-/-}* larval fat bodies. *Desat1* mutant fat bodies show reduced lysotracker staining. Scale bars 20 μ m (B). Genotypes are: (C) *y w* (*control*, *WT*), *y*; *Atg18KG03090/Atg18KG03090* (*Atg18^{-/-}*), *y w*; *P{GD2950}* *v33338/pp-gal4*; *Df(3R)Exel7316* (*Desat1^{-/-}*).

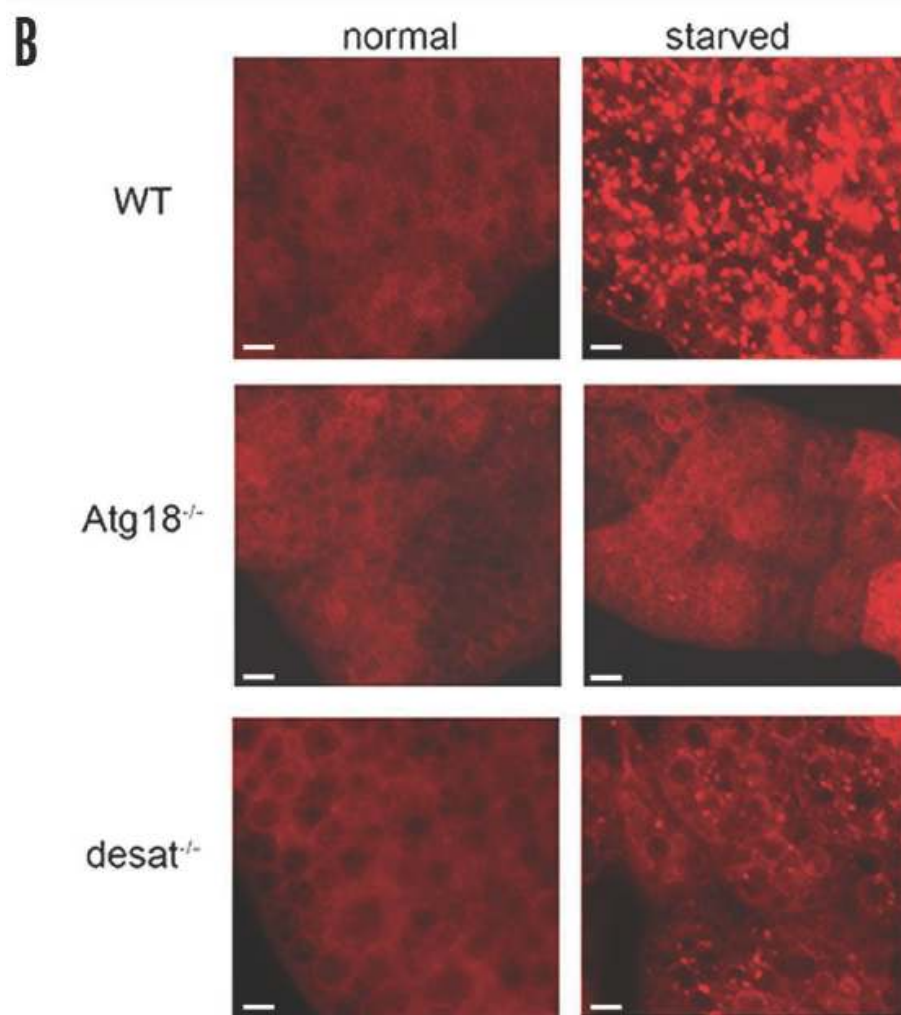
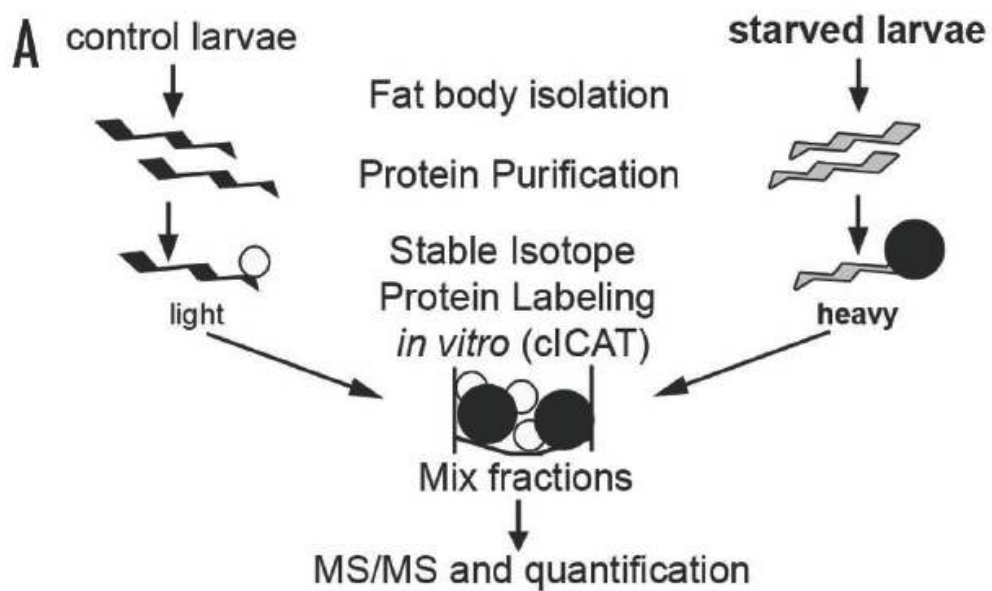


Figure 2. Generation of *Desat1* deletions. (A) *Desat1* deletion alleles obtained in the jumpout screen mobilizing P{EPgy2}*desat1*EY07679. UTRs are shown in white and ORFs in black. Deletions are indicated with grey lines. Asterisks mark the alternative ATGs. (B) Phenotype of homozygous mutant larvae. The mutants 11A and 119A are small, arrest development at larval stage 2 and die 2 days later. Mutants 28B are viable without obvious phenotypes. (C) *Desat1* protein expression in homozygous mutant larvae. Only mutant 28B produces *Desat1* protein, but a shorter version of 32 kDa. Genotypes are: *y w*; P{EPgy2}*desat1*EY07679, *y w*; *Desat10/Desat10* (control), *y w*; *Desat11/Desat11*, *y w*; *Desat119/Desat119*, *y w*; *Desat 28/Desat28*.

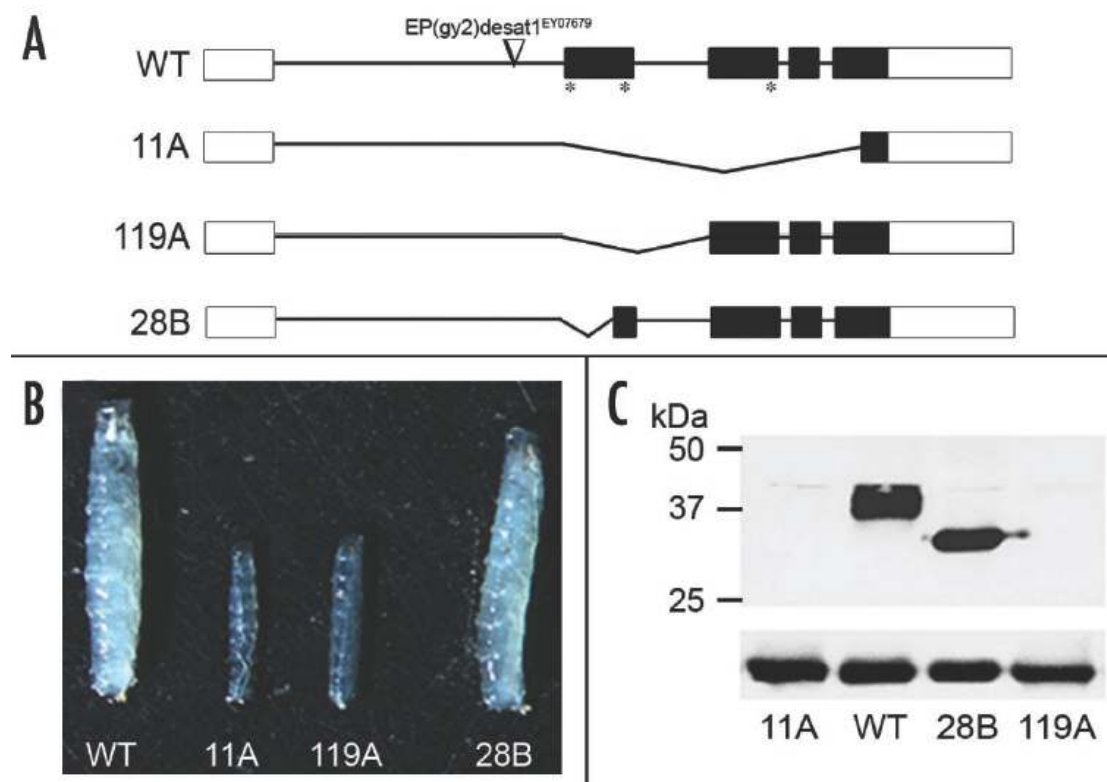


Figure 3. Desat1 is involved in autophagic processes. (A–A'') Desat1 mutant clones fail to incorporate lysotracker. Fat body clones mutant for Desat1 were generated using the FRT-FLP technique and stained with lysotracker after 4 h of sucrose starvation. The Desat1 mutant clones (marked by the absence of GFP) display reduced lysotracker staining compared to the surrounding WT cells. (B–B'') Loss of Desat1 function affects the distribution of Atg8. Fat body clones mutant for Desat1 were generated using the FRT-FLP technique in an RFP-Atg8 expressing background. Cells lacking Desat1 function (marked by the absence of GFP) exhibit mostly cytoplasmic localization of Atg8 compared to the surrounding WT cells. (C and D) Desat1 mutant fat bodies do not accumulate autophagosomal vesicles upon starvation. Shown are TEM pictures of control (precise excision of P-element, C and C') and Desat1 mutant (D and D') fat bodies. The inset in (D') shows a magnification of the vesicles prominent in Desat1 mutant cells. Autolysosomes are marked by arrows, and lysosomes by arrowheads, respectively. (E) Autophagic structures are strongly decreased in Desat1 mutant cells. Scale bars 20 μ m (A–A'' and B–B''), 5 μ m (C and D), 0.5 μ m (C' and D'), 0.2 μ m (inset D'). Genotypes are: (A) *y w hsflp; FRT82-Desat11/FRT82-UbiGFP*, (B) *y w hsflp; RFP-ATG8/pp1-gal4; FRT82-Desat11/FRT82-UbiGFP*, (C–E) *y w; Desat10/Desat10, y w; Desat11/Desat11*.

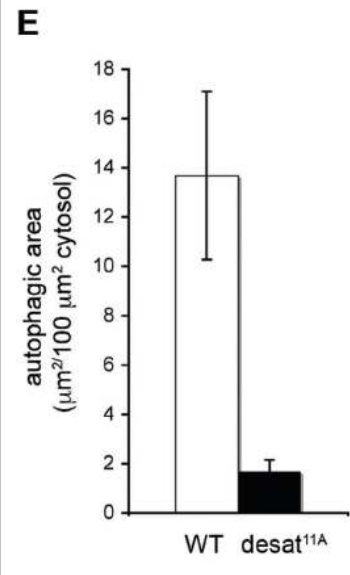
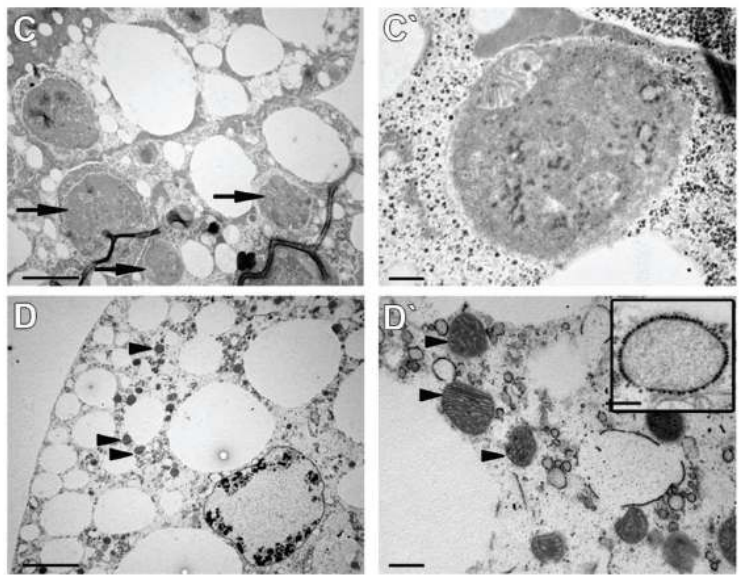
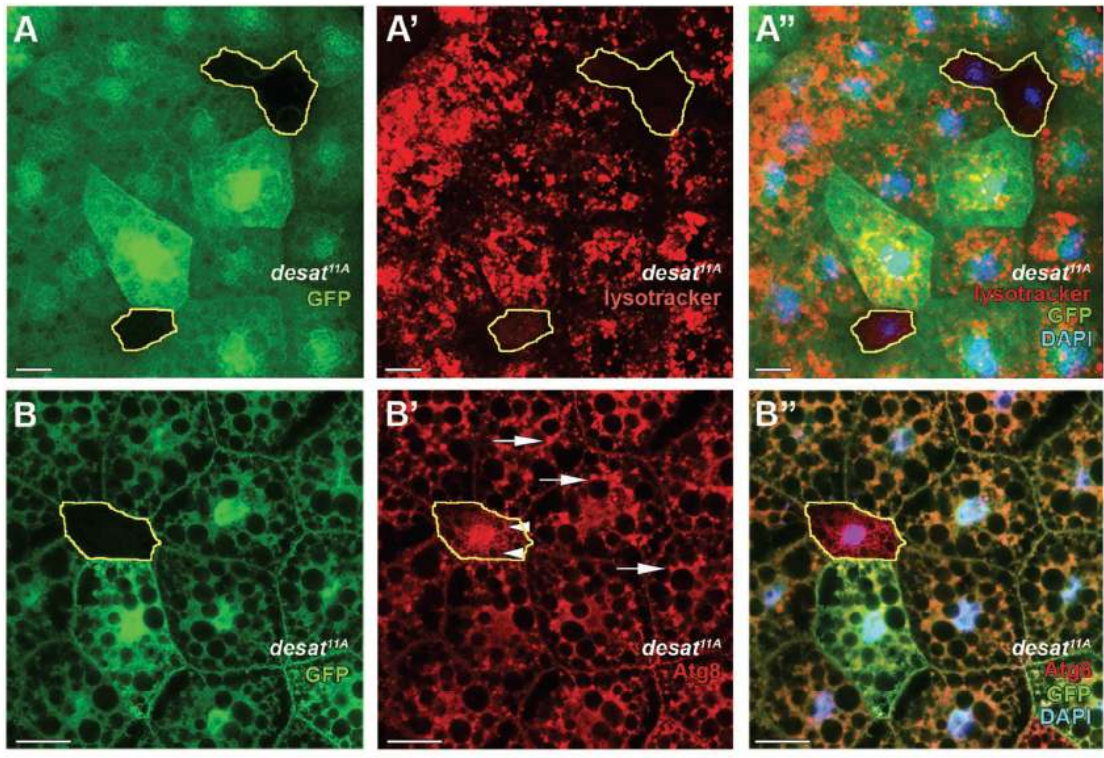


Figure 4. Intracellular distribution of Desat1 protein in S2 cells under starvation. HA-tagged Desat1 partially colocalizes with GFP-ATG5 (A–A'') or GFPATG8 (B–B'') upon PBS starvation. Scale bar 10 μ m.

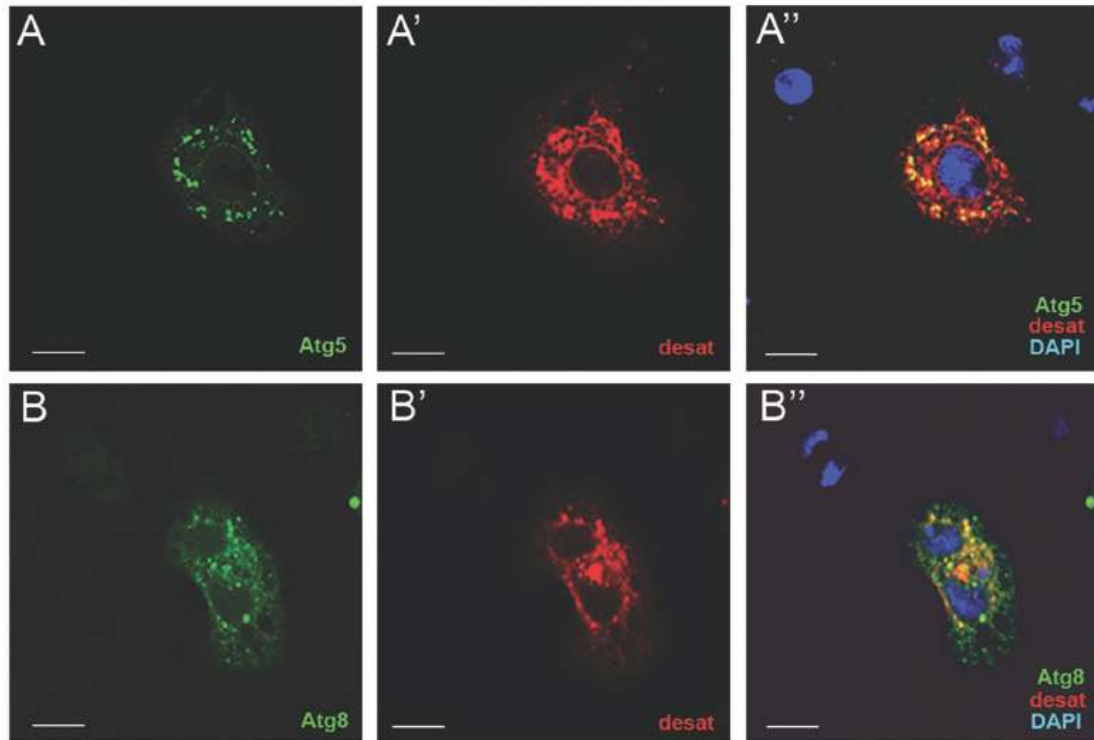


Figure 5. Desat1 mutation affects lipid compositions and the degree of unsaturation of major fly phospholipids. (A–C) The major fly phospholipids PE, PI and PC were quantified by MMR. Relative quantities of each molecular species was calculated by the log10ratio (mutant/wt) intensities and plotted as a heat map with darker shades indicating an increase and light shades indicating a decrease in the respective ions. (B' and C'): Fatty acid analysis of PE and PI species reveal a decrease in unsaturated lipid species in Desat1 mutants (black bars) compared to WT larvae (light bars). (D) Ceramide and PE-ceramide levels are increased in Desat1 mutants (black bars) compared to WT larvae (light bars). Genotypes are: *y w*; *desat10/desat10* (WT), *y w*; *desat11A/desat11A*.

